BBVA Research

Creating Opportunities

N.º 25/04
Working Paper

Unraveling the impact of a carbon price shock on macroeconomic variables: a Narrative Sign Restrictions approach

Joxe Mari Barrutiabengoa Ortubai,
Rodrigo Enrique Falbo Piacentini,
Agustín García Serrador,
Juan F. Rubio-Ramírez

April 2025

Unraveling the impact of a carbon price shock on macroeconomic variables: a Narrative Sign Restrictions approach

Joxe Mari Barrutiabengoa Ortubai
BBVA Research

Rodrigo Enrique Falbo Piacentini
BBVA Research

Agustín García Serrador
BBVA Research

Juan F. Rubio-Ramírez*
Emory University and BBVA Research

Abstract

This paper investigates the macroeconomic effects of carbon price shocks using a Structural Vector Autoregression (SVAR) framework identified through Narrative Sign Restrictions. This identification strategy streamlines the modeling process by anchoring the analysis to key regulatory events, thereby obviating the need for explicitly defined shock variables. Focusing on the European Union Emissions Trading System (EU-ETS), the paper also improves the identification of carbon price shocks by addressing their frequent conflation with concurrent demand-side disturbances. The results suggest that carbon price shocks have a more substantial impact on economic activity than previously indicated by the literature on other carbon policy instruments. However, the estimated effects are more moderate than those reported in recent studies of the EU-ETS, which find an elasticity close to one between emissions and output. The findings also reinforce the effectiveness of carbon pricing as a policy tool to achieve significant reductions in greenhouse gas (GHG) emissions.

Keywords: Narrative information, SVARs, Bayesian approach, sign restrictions, carbon price, EU-ETS, decarbonization.
JEL Classification Numbers: C32, E32, E52, F44, Q54, Q58.

*Corresponding author: Juan F. Rubio-Ramírez <juan.rubio-ramirez@emory.edu>, Economics Department, Emory University, Rich Memorial Building, Room 306, Atlanta, Georgia 30322-2240.

1 Introduction

The growing threat of climate change highlights the urgent need for policies that reduce greenhouse gas (GHG) emissions. As of November 2024, Project (2024) estimates that the remaining carbon budget (RCB) -the total amount of CO2 that can be emitted without surpassing critical warming thresholds- is approximately 235 GtCO2 for a 50% probability of limiting global warming to 1.5°C. This corresponds to roughly six years of emissions at current rates. For a 50% chance of remaining below 2°C, the RCB is around 1,110 GtCO2, equivalent to approximately 27 years of emissions. Absent decisive mitigation efforts, the objective of the Paris Agreement -to limit warming to well below 2ºC by 2100- may become increasingly unattainable.

In this context, carbon pricing has emerged as a cornerstone policy instrument for addressing the negative externalities associated with emissions. By internalizing the social costs of carbon into individual decision-making, carbon pricing aims to align private incentives with broader societal objectives. However, accurately estimating the social cost of carbon remains challenging, as it depends on assumptions regarding physical damages, economic modeling frameworks, and the choice of discount rates (Moore et al., 2024).

The Paris Agreement, signed by 196 parties in 2016, adopts a precautionary approach, aiming to limit global warming well below 2°C in order to mitigate the risk of catastrophic climate outcomes. In this context, Pindyck (2022) characterizes climate change mitigation as a form of insurance against potentially severe economic disruptions, which, under extreme warming scenarios, could lead to GDP losses ranging from 20 to 40%. While limiting temperature increases is critical to averting such outcomes, achieving these targets within a narrow time horizon may involve substantial economic trade-offs, as reaching net-zero emissions will require reversing decades of cumulative emission growth within just a couple of decades -a formidable and costly undertaking.

Recent analyses suggest a high elasticity between emissions and economic activity in the European Union, implying that decarbonization efforts may inherently slow economic growth. Känzig (2024) reports an elasticity that exceeds one, indicating that emission reductions triggered by regulatory events are associated with even greater contractions in output. However, this finding is difficult to reconcile with the long-run decline in both energy intensity (energy consumption per unit of GDP) and emissions intensity (emissions per unit of energy), which has occurred alongside sustained economic growth across Europe. This apparent inconsistency may stem from identification challenges, particularly the conflation of carbon policy impacts with concurrent negative demand shocks.

This paper advances the literature on the economic effects of carbon price policies by introducing a refined methodology that improves the identification of carbon price shocks and disentangles them from other concurrent disturbances. Specifically, it integrates Känzig (2024)'s carbon policy surprise framework with Narrative Sign Restrictions (NSR) within a Structural Vector Autoregression (SVAR) model. By focusing on the most representative regulatory events, the approach mitigates biases arising from overlapping demand-side shocks and eliminates the need for explicitly constructed shock variables, thereby streamlining the modeling strategy. This innovation not only enhances the precision of shock identification, but also yields results that are consistent with key economic episodes and narratives, including the Global Financial Crisis and the COVID-19 pandemic.

The rest of this paper is organized as follows. Section 2 provides an overview of the EU Emissions Trading System (EU ETS) and the evolution of GHG emissions in the European Union, highlighting key developments and recent trends. Section 3 reviews recent literature on the macroeconomic effects of carbon pricing instruments. Sections 4 to 6 outline the foundational SVAR framework and detail the incorporation of narrative information through sign restrictions. Section 7 applies this methodology to the EU ETS market, while Section 8 evaluates its effects on European economic activity. We simulate the potential impacts of a net-zero scenario aligned with Phase IV of the Network for Greening the Financial System (NGFS). Finally, Section 9 concludes.

2 Carbon emissions and schemes in the EU

2.1 The evolution of GHG emissions

The evolution of GHG in the European Union can be contextualized through the Kaya identity, which decomposes total emissions into four fundamental drivers: population, GDP per capita, energy intensity (energy consumption per unit of GDP), and carbon intensity (GHG emissions per unit of energy). Formally, the identity is expressed as:

$$\text{GHG emis.} = \text{Population} \times \left(\frac{\text{GDP}}{\text{Population}}\right) \times \left(\frac{\text{Energy cons.}}{\text{GDP}}\right) \times \left(\frac{\text{GHG emis.}}{\text{Energy cons.}}\right)$$

which simplifies to:

$$\text{GHG emis.} = \text{GDP} \times \left(\frac{\text{Energy cons.}}{\text{GDP}}\right) \times \left(\frac{\text{GHG emis.}}{\text{Energy cons.}}\right)$$

As illustrated in Figure 1, the evolution of EU GHG emissions since 1990 can be broadly characterized by three distinct phases of decarbonization. From 1990 to 2005, emissions remained relatively flat, declining at an annual average rate of just 0.3%. During this period, GDP growth largely offset modest gains in energy efficiency and carbon intensity. Between 2005 and 2018, emissions fell more substantially, with an average annual reduction of 1.5%, driven primarily by accelerated improvements in energy intensity and, to a lesser extent, cleaner energy production. Since 2018, the pace of decarbonization has increased, with emissions dropping by an average of 3.1% per year. This recent phase reflects significant strides in energy efficiency, partly spurred by geopolitical developments, such as the reduced reliance on Russian natural gas, and the rapid deployment of renewable energy technologies. However, sustained GDP growth continues to partially offset emission reductions, underscoring the critical importance of decoupling economic activity from GHG emissions.

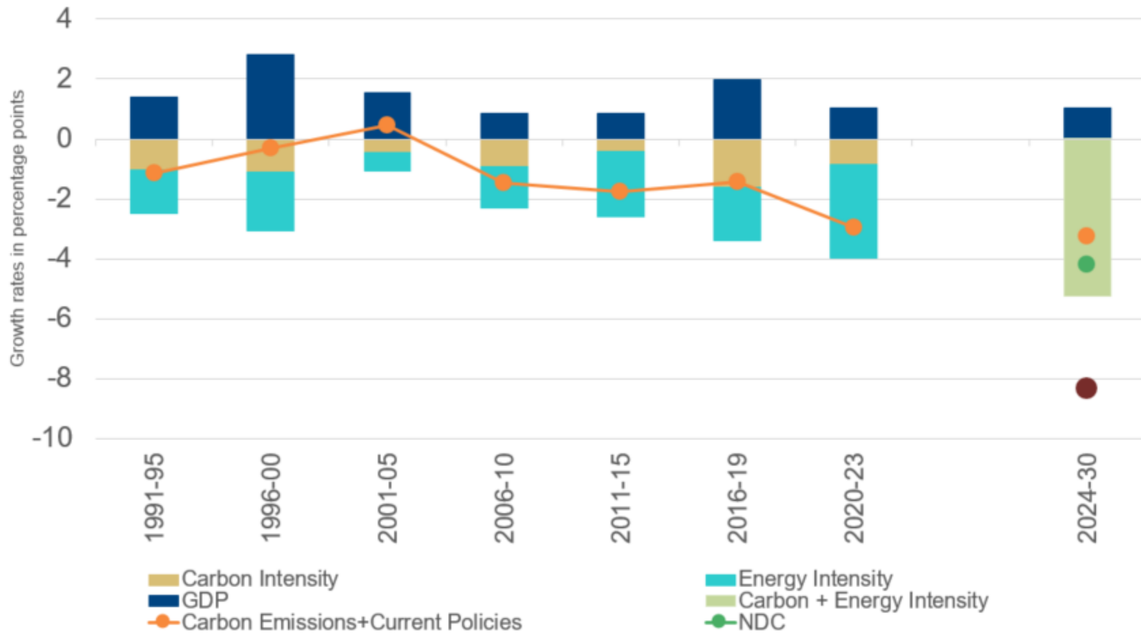

Figure 1: *GHG emissions, EU. Kaya's identity.*

Despite recent reductions, current GHG emissions trajectories remain insuficient to meet both the EU's Nationally Determined Contribution (NDC) and net-zero pathways, underscoring the need for unprecedent policy action or technological innovation. Figure 1 displays in the final column the projected emissions (2024–2030) by Tracker (2024) in an escenario without additional policies, alongside the reductions required to meet both the NDC targets (green dot) and net-zero goals (brown dot). Specifically, assuming a continued annual growth rate of approximately 1%, achieving these targets would demand unprecedented declines in carbon and energy intensity, even for the NDC scenario, as evidenced by the light green column.

2.2 The EU-ETS: evolution and challenges

The European Union Emissions Trading System (EU-ETS) is the world's most comprehensive pricing instrument, covering approximately 40% of the EU's GHG emissions as of 2024. Since its inception in 2005, the EU-ETS has undergone several reforms to align with the EU's climate goals. The first phase (2005-2007) served as a pilot but was undermined by a significant oversupply of free allowances. The second phase (2008-2012) introduced stricter rules, including reduced free allocations and broader coverage, but faced challenges from the 2008 financial crisis. The third phase (2013-2020) introduced pivotal reforms, such as the centralized auctioning of the allowances, stricter regulations on the power sector, and a market stability reserve to manage supply imbalances. The ongoing fourth phase (2021-2030) accelerates efforts with a sharper emissions cap reduction, expanded sector coverage, and measures to address carbon leakage, aligning the system more closely with the EU's long-term climate objectives (Commission, 2025).

It is important to note that the EU-ETS has historically prioritized regulating CO2 emissions, particularly from energy-intensive sectors. The system's design has primarily targeted industries such as power generation, aviation, and manufacturing (e.g. cement or steel), which collectively account for a substantial share of EU-wide CO2 output. In contrast, non-CO2 greenhouse gases (e.g., methane from agriculture) have remained largely excluded from the scope of the system. Similarly, emissions from sectors like road transport and buildings, key contributors to the EU's carbon footprint, have thus far been excluded and are scheduled to be only partially integrated into the EU-ETS 2 framework starting in 2027. This selective scope underscores both the system's effectiveness in driving decarbonization within industrial processes and its limitations in addressing the full spectrum of EU emissions.

While the EU-ETS appears at first glance to be effective in reducing carbon emissions, see

Figure 2, its broader macroeconomic effects remain a matter of intense debate[1]. Assessing the economic consequences of a carbon price shock -whether on output, employment, inflation, or macroeconomic stability- presents significant challenges. Historical data are confounded by the overlapping occurrence of major economic disruptions and pivotal regulatory reforms in the EU-ETS, making it challenging to isolate and accurately measure the individual impacts of its multiple structural changes. For instance, the 2008 Global Financial Crisis and the economic disruptions caused by the COVID-19 pandemic coincided with key regulatory adjustments in the EU-ETS, thereby complicating efforts to disentangle the impact of carbon pricing from those of contemporaneous economic shocks.

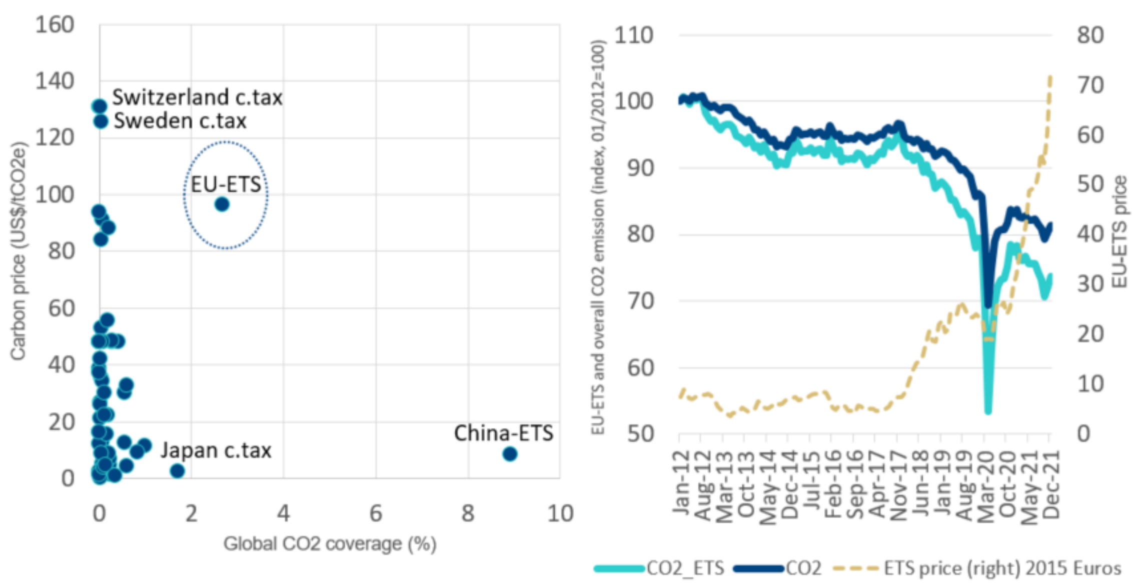

Figure 2: *Graph in the left: Carbon price instruments, 2023. Graph in the right: EU CO2 emissions, 2012-2021.*

[1]Regarding the more pronounced decline in emissions within the EU ETS compared to the overall EU emissions, it is theoretically possible that factors beyond emissions pricing, such as variations in demand effects, may explain this divergence.

3 Literature review

The impact of carbon pricing, particularly the EU-ETS, on emissions and macroeconomic variables has become a central topic in environmental economics. Foundational studies, such as Martin et al. (2014) and Andersson (2019), provide robust evidence that carbon pricing is effective in reducing emissions. However, its broader macroeconomic implications have only recently begun to receive systematic attention in the literature.

Theoretical models, including McKibbin et al. (2017) and Goulder and Hafstead (2018), generally predict contractionary effects on output. In contrast, empirical studies such as Metcalf (2019) and Bernard and Kichian (2021) find negligible impacts of carbon taxes on GDP, suggesting that well-designed mechanisms may avoid significant economic damage. Metcalf and Stock (2020) and Konradt and Weder di Mauro (2021) extend this analysis to employment and inflation, finding no major adverse effects in European and Canadian carbon pricing systems. However, the relatively modest scope and tax rates of many carbon pricing schemes -as well as the presence of offsetting fiscal measures- may mask the true macroeconomic impacts.

Recent research has increasingly focused on the distributional effects of carbon pricing. Ohlendorf et al. (2021) highlight the disproportionate burden borne by lower-income households in the EU, while Hensel et al. (2024) link carbon price shocks to shifts in inflation expectations. National and firm-level responses also vary, with Berthold et al. (2023) finding greater economic disruption in carbon-intensive economies, and Känzig and Konradt (2023) identifying institutional factors like free permit allocation and market structure as key determinants of policy effectiveness.

A significant contribution comes from Känzig (2024), who isolates regulatory-driven carbon price shocks within the EU-ETS, revealing persistent increases in consumer prices and reduced economic activity. Building on his methodology, this paper refines the identification of carbon price shocks and provides more precise estimates of their macroeconomic effects. While reducing the green premium entails transitional costs, the results are consistent with the expectation of temporary economic disruptions until green technologies reach full deployment. Intuitively, carbon pricing mechanisms aimed at decarbonization effectively shorten the productive lifespan of capital assets originally designed for a carbon-intensive economy. By increasing the real cost of utilizing such capital, these mechanisms accelerate the reallocation of economic activities and alter spending and saving decisions, potentially dampening aggregate economic performance.

4 The Model

Consider the structural vector autoregression of the general form

$$\mathbf{y}_t'\mathbf{A}_0 = \sum_{\ell=1}^{p} \mathbf{y}_{t-\ell}'\mathbf{A}_\ell + \mathbf{c} + \varepsilon_t' \quad \text{for } 1 \le t \le T \tag{1}$$

where $\mathbf{y}_t$ is an $n \times 1$ vector of variables, ε_t is an $n \times 1$ vector of structural shocks, $\mathbf{A}_\ell$ is an $n \times n$ matrix of parameters for $0 \le \ell \le p$ with $\mathbf{A}_0$ invertible, $\mathbf{c}$ is a $1 \times n$ vector of parameters, p is the lag length, and T is the sample size. The vector ε_t, conditional on past information and the initial conditions $\mathbf{y}_0, \ldots, \mathbf{y}_{1-p}$, is Gaussian with mean zero and covariance matrix $\mathbf{I}_n$, the $n \times n$ identity matrix. The model described in Equation (1) can be written as

$$\mathbf{y}_t'\mathbf{A}_0 = \mathbf{x}_t'\mathbf{A}_+ + \varepsilon_t' \quad \text{for } 1 \le t \le T, \tag{2}$$

where $\mathbf{A}_+' = \begin{bmatrix} \mathbf{A}_1' & \cdots & \mathbf{A}_p' & \mathbf{c}' \end{bmatrix}$ and $\mathbf{x}_t' = \begin{bmatrix} \mathbf{y}_{t-1}', \ldots, \mathbf{y}_{t-p}', 1 \end{bmatrix}$ for $1 \le t \le T$. The dimension of $\mathbf{A}_+$ is $m \times n$ and the dimension of $\mathbf{x}_t$ is $m \times 1$, where $m = np + 1$. The reduced-form representation implied by Equation (2) is

$$\mathbf{y}_t' = \mathbf{x}_t'\mathbf{B} + \mathbf{u}_t' \text{ for } 1 \leq t \leq T,$$

where $\mathbf{B} = \mathbf{A}_+\mathbf{A}_0^{-1}$, $\mathbf{u}_t' = \varepsilon_t'\mathbf{A}_0^{-1}$, and $\mathbb{E}\left[\mathbf{u}_t\mathbf{u}_t'\right] = \mathbf{\Sigma} = \left(\mathbf{A}_0\mathbf{A}_0'\right)^{-1}$. The matrices $\mathbf{B}$ and $\mathbf{\Sigma}$ are the reduced-form parameters, while $\mathbf{A}_0$ and $\mathbf{A}_+$ are the structural parameters. Similarly, $\mathbf{u}_t'$ are the reduced-form innovations, while ε_t' are the structural shocks. The shocks are orthogonal and have an economic interpretation, while the innovations are, in general, correlated and do not have an interpretation. Let $\mathbf{\Theta} = (\mathbf{A}_0, \mathbf{A}_+)$ collect the value of the structural parameters.

4.1 Impulse responses

Recall the definition of impulse responses. Given a value $\mathbf{\Theta}$ of the structural parameters, the response of the i-th variable to the j-th structural shock at horizon k corresponds to the element in row i and column j of the matrix $\mathbf{L}_k(\mathbf{\Theta})$, where $\mathbf{L}_k(\mathbf{\Theta})$ is defined recursively by

$$\mathbf{L}_0(\mathbf{\Theta}) = \left(\mathbf{A}_0^{-1}\right)', \quad \mathbf{L}_k(\mathbf{\Theta}) = \sum_{\ell=1}^{k}\left(\mathbf{A}_\ell\mathbf{A}_0^{-1}\right)'\mathbf{L}_{k-\ell}(\mathbf{\Theta}), \text{ for } 1 \leq k \leq p,$$
$$\mathbf{L}_k(\mathbf{\Theta}) = \sum_{\ell=1}^{p}\left(\mathbf{A}_\ell\mathbf{A}_0^{-1}\right)'\mathbf{L}_{k-\ell}(\mathbf{\Theta}), \text{ for } p < k < \infty.$$

Given a value $\mathbf{\Theta}$ of the structural parameters and the data, the structural shocks at time t are

$$\varepsilon_t'(\mathbf{\Theta}) = \mathbf{y}_t'\mathbf{A}_0 - \mathbf{x}_t'\mathbf{A}_+ \text{ for } 1 \leq t \leq T. \tag{3}$$

5 The Identification Problem and Sign Restrictions

As is well known, the structural form in Equation (1) is not identified, so restrictions must be imposed on the structural parameters to solve the identification problem. The desire to impose only minimalist identification restrictions that are agreed upon by most researchers motivated Faust (1998); Canova and Nicolo (2002); Uhlig (2005); Rubio-Ramirez et al. (2010) to develop methods to identify the structural parameters by placing a handful of uncontroversial traditional sign restrictions on the impulse responses or the structural parameters themselves. Antolín-Díaz and Rubio-Ramírez (2018) developed a new class of sign restrictions based on narrative information that they call Narrative Sign Restrictions. NSR constrains the structural parameters by ensuring that around a handful of key historical events, the structural shocks, and/or historical decompositions agree with the established narrative. In this paper, we combine traditional and narrative sign restrictions to identify EU-ETS carbon price shocks in the main macroeconomic variables.

5.1 Traditional sign restrictions

Traditional sign restrictions are well understood and their use is widespread in the literature. In particular, Rubio-Ramirez et al. (2010) highlights how this class of restrictions can be characterized by the function

$$\Gamma(\mathbf{\Theta}) = \left(\mathbf{e}'_{1,n}\mathbf{F}(\mathbf{\Theta})'\mathbf{S}'_1, \cdots, \mathbf{e}'_{n,n}\mathbf{F}(\mathbf{\Theta})'\mathbf{S}'_n\right)' > \mathbf{0}. \tag{4}$$

Appropriate choices of $\mathbf{S}_j$ and $\mathbf{F}(\mathbf{\Theta})$ will lead to sign restrictions on the impulse responses or the structural parameters themselves. In particular, to impose restrictions on the impulse responses, one can define $\mathbf{F}(\mathbf{\Theta})$ as vertically stacking the impulse responses at the different horizons over which we want to impose the restrictions and $\mathbf{S}_j$ as an $s_j \times r_j$ matrix of zeros, ones and negative ones that will select the horizons and the variables over which we want to impose the r_j sign restrictions to identify structural shock j. If instead we want to impose restrictions on the structural parameters themselves, we can then define $\mathbf{F}(\mathbf{\Theta}) = \mathbf{\Theta}$ and $\mathbf{S}_j$ as an $s_j \times r_j$ matrix of zeros, ones and negative ones that will select entries of $\mathbf{\Theta}$ over which we want to impose the sign restrictions.

5.2 Narrative sign restrictions

Antolín-Díaz and Rubio-Ramírez (2018) consider two types of NSR. First, restrictions on the signs of structural shocks. Second, restrictions on the historical decomposition. The approach of this paper relies on the first one.

5.2.1 Restrictions on the signs of the structural shocks

Let us assume that we want to impose the restriction that the signs of the j-th shock at s_j episodes occurring at dates $t_1, \ldots, t_{s_j}$ are all positive. Then, the NSR can be imposed as

$$\mathbf{e}'_{j,n} \varepsilon_{t_v} (\mathbf{\Theta}) > 0 \text{ for } 1 \leq v \leq s_j. \tag{5}$$

Assume instead that we want to impose the restriction that the signs of the j-th shock at s_j episodes occurring at dates $t_1, \ldots, t_{s_j}$ are negative. Then, the NSR can be imposed with a negative sign on the left-hand side of Equation (5). Of course, one could restrict the shocks in a few periods to be negative and positive in a few others.

6 Bayesian Inference

In this section, we describe how to perform Bayesian inference to handle NSR. Equations (5) imply the following function to characterize NSR

$$\phi\left(\boldsymbol{\Theta}, \varepsilon^{v}\right) > \mathbf{0}, \tag{6}$$

where $\varepsilon^{v} = \left(\varepsilon_{t_1}, \ldots, \varepsilon_{t_v}\right)$ are the structural shocks constrained by the NSR. A comparison with Equation (4) makes it clear that the traditional sign restrictions depend on the structural parameters, whereas the NSR depends as well on the structural shocks. Moreover, Equation (3) implies the following invertible function

$$\varepsilon_t = g_h\left(\mathbf{y}_t, \mathbf{x}_t, \boldsymbol{\Theta}\right) \text{ for } 1 \leq t \leq T, \tag{7}$$

with $\mathbf{y}_t = g_h^{-1}\left(\varepsilon_t; \mathbf{x}_t, \boldsymbol{\Theta}\right)$ for $1 \leq t \leq T$. Using Equations (6) and (7), we can write

$$\tilde{\phi}\left(\boldsymbol{\Theta}, \mathbf{y}^{v}, \mathbf{x}^{v}\right) = \phi\left(\boldsymbol{\Theta}, g_h\left(\mathbf{y}_{t_1}, \mathbf{x}_{t_1}, \boldsymbol{\Theta}\right), \ldots, g_h\left(\mathbf{y}_{t_v}, \mathbf{x}_{t_v}, \boldsymbol{\Theta}\right)\right) > \mathbf{0}, \tag{8}$$

where $\mathbf{y}^{v} = \left(\mathbf{y}_{t_1}, \ldots, \mathbf{y}_{t_v}\right)$ and $\mathbf{x}^{v} = \left(\mathbf{x}_{t_1}, \ldots, \mathbf{x}_{t_v}\right)$. Hence, given the data, Equation (6) is continuous on the structural parameters while, given the structural parameters, Equation (6) is continuous on the structural shocks.

6.1 The posterior distribution

We can consider an alternative parameterization of the structural VAR in (2), defined by $\mathbf{B}$, $\boldsymbol{\Sigma}$, and $\mathbf{Q}$, where $\mathbf{Q} \in O(n)$, the set of all orthogonal $n \times n$ matrices, which we call the orthogonal reduced-form parameterization. To define a mapping between $\boldsymbol{\Theta}$ and $(\mathbf{B}, \boldsymbol{\Sigma}, \mathbf{Q})$, one must first choose a decomposition of the covariance matrix $\boldsymbol{\Sigma}$. Let $h(\boldsymbol{\Sigma})$ be an $n \times n$ matrix that satisfies $h(\mathbf{\Sigma})'h(\mathbf{\Sigma}) = \mathbf{\Sigma}$, where h is differentiable. One would normally choose $h(\mathbf{\Sigma})$ to be the Cholesky decomposition. Given a decomposition h, we can define the mapping between $\mathbf{\Theta}$ and $(\mathbf{B}, \mathbf{\Sigma}, \mathbf{Q})$

$$f_h(\mathbf{\Theta}) = (\underbrace{\mathbf{A}_+\mathbf{A}_0^{-1}}_{\mathbf{B}}, \underbrace{(\mathbf{A}_0\mathbf{A}_0')^{-1}}_{\mathbf{\Sigma}}, \underbrace{h((\mathbf{A}_0\mathbf{A}_0')^{-1})\mathbf{A}_0}_{\mathbf{Q}}),$$

where it is easy to see that $h((\mathbf{A}_0\mathbf{A}_0')^{-1})\mathbf{A}_0$ is an orthogonal matrix. The function f_h is invertible, with inverse defined by

$$f_h^{-1}(\mathbf{B}, \mathbf{\Sigma}, \mathbf{Q}) = (\underbrace{h(\mathbf{\Sigma})^{-1}\mathbf{Q}}_{\mathbf{A}_0}, \underbrace{\mathbf{B}h(\mathbf{\Sigma})^{-1}\mathbf{Q}}_{\mathbf{A}_+}). \tag{9}$$

Using Equation (9), we can rewrite Equation (8) as $\Phi(\mathbf{B}, \mathbf{\Sigma}, \mathbf{Q}, \mathbf{y}^v, \mathbf{x}^v) = \tilde{\phi}\left(f_h^{-1}(\mathbf{B}, \mathbf{\Sigma}, \mathbf{Q}), \mathbf{y}^v, \mathbf{x}^v\right) > \mathbf{0}$. Thus, the posterior of $(\mathbf{B}, \mathbf{\Sigma}, \mathbf{Q})$ subject to the NSR is

$$\pi\left(\mathbf{B}, \mathbf{\Sigma}, \mathbf{Q}|\mathbf{y}^T, \Phi(\mathbf{B}, \mathbf{\Sigma}, \mathbf{Q}, \mathbf{y}^v, \mathbf{x}^v) > \mathbf{0}\right) = \frac{\pi\left(\mathbf{y}^T|\mathbf{B}, \mathbf{\Sigma}, \mathbf{Q}, \Phi(\mathbf{B}, \mathbf{\Sigma}, \mathbf{Q}, \mathbf{y}^v, \mathbf{x}^v) > \mathbf{0}\right)\pi\left(\mathbf{B}, \mathbf{\Sigma}, \mathbf{Q}\right)}{\int \pi\left(\mathbf{y}^T|\mathbf{B}, \mathbf{\Sigma}, \mathbf{Q}, \Phi(\mathbf{B}, \mathbf{\Sigma}, \mathbf{Q}, \mathbf{y}^v, \mathbf{x}^v) > \mathbf{0}\right)\pi\left(\mathbf{B}, \mathbf{\Sigma}, \mathbf{Q}\right) d\left(\mathbf{B}, \mathbf{\Sigma}, \mathbf{Q}\right)}, \tag{10}$$

where $\mathbf{y}^T = \{\mathbf{y}_{1-p}, \ldots, \mathbf{y}_0, \ldots, \mathbf{y}_T\}$ is the data, $\pi\left(\mathbf{y}^T|\mathbf{B}, \mathbf{\Sigma}, \mathbf{Q}, \Phi(\mathbf{B}, \mathbf{\Sigma}, \mathbf{Q}, \mathbf{y}^v, \mathbf{x}^v) > \mathbf{0}\right)$ is the likelihood function subject to the NSR and $\pi\left(\mathbf{B}, \mathbf{\Sigma}, \mathbf{Q}\right)$ is the prior. Antolín-Díaz and Rubio-Ramírez (2018) show that the truncated likelihood function in Equation (10) can be written as

$$\pi\left(\mathbf{y}^T|\mathbf{B}, \mathbf{\Sigma}, \mathbf{Q}, \Phi\left(\mathbf{B}, \mathbf{\Sigma}, \mathbf{Q}, \mathbf{y}^v, \mathbf{x}^v\right) > \mathbf{0}\right) = \frac{[\Phi(\mathbf{B},\mathbf{\Sigma},\mathbf{Q},\mathbf{y}^v,\mathbf{x}^v)>\mathbf{0}]\pi\left(\mathbf{y}^T|\mathbf{B},\mathbf{\Sigma}\right)}{\omega(\mathbf{B},\mathbf{\Sigma},\mathbf{Q})}, \tag{11}$$

where $\omega\left(\mathbf{B}, \mathbf{\Sigma}, \mathbf{Q}\right) = \int\left[\tilde{\Phi}\left(\mathbf{B}, \mathbf{\Sigma}, \mathbf{Q}, \varepsilon^v\right) > \mathbf{0}\right]\left(\prod_{s=1}^{v}\pi\left(\varepsilon_{t_s}\right)\right) d\left(\varepsilon_{t_1}\ldots\varepsilon_{t_v}\right)$. Equation (11) makes clear that the truncated likelihood can be written as a re-weighting of the likelihood function, with weights inversely proportional to the probability of satisfying the restriction.

One would normally choose priors of $(\mathbf{B}, \mathbf{\Sigma}, \mathbf{Q})$ that are uniform over $O(n)$. When that is the case, $\pi(\mathbf{B}, \mathbf{\Sigma}, \mathbf{Q}) = \pi(\mathbf{B}, \mathbf{\Sigma})$, and the posterior of $(\mathbf{B}, \mathbf{\Sigma}, \mathbf{Q})$ subject to the NSR is proportional to

$$\pi\left(\mathbf{B}, \mathbf{\Sigma}, \mathbf{Q} | \mathbf{y}^T, \Phi(\mathbf{B}, \mathbf{\Sigma}, \mathbf{Q}, \mathbf{y}^v, \mathbf{x}^v) > \mathbf{0}\right) \propto \frac{[\Phi(\mathbf{B}, \mathbf{\Sigma}, \mathbf{Q}, \mathbf{y}^v, \mathbf{x}^v) > \mathbf{0}]\, \pi\left(\mathbf{y}^T | \mathbf{B}, \mathbf{\Sigma}\right)}{\omega(\mathbf{B}, \mathbf{\Sigma}, \mathbf{Q})} \pi(\mathbf{B}, \mathbf{\Sigma}).$$

In other words, the posterior distribution is proportional to the re-weighted likelihood times the prior. On the contrary, as mentioned above, in the case of traditional sign restrictions, it is the prior and not the likelihood that is truncated. Using similar derivations, under priors that are uniform over $O(n)$ the posterior distribution subject to the traditional sign restrictions is $\pi\left(\mathbf{B}, \mathbf{\Sigma}, \mathbf{Q} | \mathbf{y}^T, \Gamma\left(f_h^{-1}(\mathbf{B}, \mathbf{\Sigma}, \mathbf{Q})\right) > \mathbf{0}\right) \propto \left[\Gamma\left(f_h^{-1}(\mathbf{B}, \mathbf{\Sigma}, \mathbf{Q})\right) > \mathbf{0}\right] \pi\left(\mathbf{y}^T | \mathbf{B}, \mathbf{\Sigma}\right) \pi(\mathbf{B}, \mathbf{\Sigma})$, in which no re-weighting of the likelihood is needed. If one uses both traditional and NSR the posterior distribution $\pi\left(\mathbf{B}, \mathbf{\Sigma}, \mathbf{Q} | \mathbf{y}^T, \Gamma\left(f_h^{-1}(\mathbf{B}, \mathbf{\Sigma}, \mathbf{Q})\right) > \mathbf{0}, \Phi(\mathbf{B}, \mathbf{\Sigma}, \mathbf{Q}, \mathbf{y}^v, \mathbf{x}^v) > \mathbf{0}\right)$ is proportional to

$$\left[\Gamma\left(f_h^{-1}(\mathbf{B}, \mathbf{\Sigma}, \mathbf{Q})\right) > \mathbf{0}\right] \frac{[\Phi(\mathbf{B}, \mathbf{\Sigma}, \mathbf{Q}, \mathbf{y}^v, \mathbf{x}^v) > \mathbf{0}]\, \pi\left(\mathbf{y}^T | \mathbf{B}, \mathbf{\Sigma}\right)}{\omega(\mathbf{B}, \mathbf{\Sigma}, \mathbf{Q})} \pi(\mathbf{B}, \mathbf{\Sigma}).$$

6.2 The algorithm

In practice, one would normally choose priors of $(\mathbf{B}, \mathbf{\Sigma}, \mathbf{Q})$ that are uniform-normal-inverse-Wishart. In that choice, we are now ready to specify our algorithm to independently draw from the uniform-normal-inverse-Wishart posterior of $(\mathbf{B}, \mathbf{\Sigma}, \mathbf{Q})$ conditional on the traditional and NSR.

Algorithm 1. *This algorithm makes independent draws from the uniform-normal-inverse-Wishart posterior of* $(\mathbf{B}, \mathbf{\Sigma}, \mathbf{Q})$ *conditional on the traditional and NSR.*

1. *Independently draw* $(\mathbf{B}, \mathbf{\Sigma})$ *from the normal-inverse-Wishart posterior of the reduced-*

form parameters and $\mathbf{Q}$ *from the uniform distribution over* $O(n)$.

2. *Check whether* $\left[\Gamma\left(f_h^{-1}(\mathbf{B},\boldsymbol{\Sigma},\mathbf{Q})\right) > \mathbf{0}\right]$ *and* $\left[\Phi\left(\mathbf{B},\boldsymbol{\Sigma},\mathbf{Q},\mathbf{y}^v,\mathbf{x}^v\right) > \mathbf{0}\right]$ *are satisfied.*

3. *If not, discard the draw. Otherwise let the importance weight of* $(\mathbf{B},\boldsymbol{\Sigma},\mathbf{Q})$ *be as follows*

   3.1. *Simulate* M *independent draws of* ε^v *from the standard normal distribution.*

   3.2. *Approximate* $\omega(\mathbf{B},\boldsymbol{\Sigma},\mathbf{Q})$ *by the proportion of the* M *draws that satisfy* $\tilde{\Phi}\left(\mathbf{B},\boldsymbol{\Sigma},\mathbf{Q},\varepsilon^v\right) > \mathbf{0}$ *and set the importance weight to* $\frac{1}{\omega(\mathbf{B},\boldsymbol{\Sigma},\mathbf{Q})}$.

4. *Return to Step 1 until the required number of draws has been obtained.*

5. *Draw with replacement from the set of* $(\mathbf{B},\boldsymbol{\Sigma},\mathbf{Q})$ *using the importance weights.*

This choice of priors of $(\mathbf{B},\boldsymbol{\Sigma},\mathbf{Q})$ is good because it is extremely easy and efficient to make independent draws from the normal-inverse-Wishart distribution and because Rubio-Ramirez et al. (2010) describes how to use the QR decomposition to independently draw the uniform distribution over $O(n)$. Algorithm 1 makes clear that it does not suffice to simply discard the draws that violate the NSR. This would imply giving higher posterior probability to draws of $(\mathbf{B},\boldsymbol{\Sigma},\mathbf{Q})$ that are more likely to satisfy the NSR. Hence, this would amount to drawing from a posterior distribution of $(\mathbf{B},\boldsymbol{\Sigma},\mathbf{Q})$ that it is not uniform-normal-inverse-Wishart. Instead, we need to compute the importance weights and re-sample the draws accordingly.[2] Also, for the reasons explained in Arias et al. (2018), Algorithm 1 is making independent draws from the posterior normal-generalized-normal distribution of $\boldsymbol{\Theta}$.[3]

[2]The number of draws M in step 3 needs to be high enough to accurately approximate the importance weights. The larger v is, the more draws will be required. We find that one thousand draws are usually enough to obtain an accurate approximation when narrative restrictions are used in one or two events. For exercises involving more than five or six restrictions, as many as one million might be needed.

[3]See Arias et al. (2018) for a definition of normal-generalized-normal distribution.

7 Model specification

In this section, we provide a detailed overview of the data, the model specification, the prior distribution, and the identification restrictions employed in the analysis. Since our approach relies on Känzig (2024)'s instrument to select the dates in which we impose the narrative sign restrictions, we also explain the construction and explanation of this variable.

7.1 Data and baseline specification

Following Känzig (2024), our baseline specification comprises eight variables. For the climate block, we include the energy component of the Harmonized Index of Consumer Prices (HICP) and total greenhouse gas (GHG) emissions. To represent the state of the economy, we incorporate the headline HICP, the industrial production index (IPI), and the unemployment rate. As Känzig (2024), given that the economy operated at the effective lower bound for much of the sample period, we employ the two-year interest rate as the key monetary policy indicator. Additionally, we include a stock market index and the Brent crude oil price (deflated by the HICP) as additional indicators. Comprehensive details on the data sources are provided in Table 1.

Figure 3 illustrates the variables included in the analysis. The sample period spans from January 1999, marking the introduction of the euro, through December 2019, consistent with Känzig (2024). All variables, except for the unemployment rate and the two-year rate, are included in log-levels multiplied by 100. The VAR is estimated on monthly data using 6 lags and a constant, weak priors on the reduced-form parameters, and a uniform distribution over the rotation matrices. The choice reflects an agnostic stance, avoiding strong assumptions about the likely values of the parameters a priori.

We successfully replicate Känzig (2024)'s results in both the internal and external

Variable	Description
HICPE	HICP energy (EA-19) 1999M1–2019M12.
GHG	Total GHG emissions excluding LULUCF and including international aviation (EU/Eurostat/own calculations) 1999M1–2019M12.
HICP	HICP all items (EA-19) 1999M1–2019M12.
IPI	Industrial production excluding construction (EA-19) 1999M1–2019M12.
CB2Y	Two-year government bond yield 1999M1–2019M12.
UNE	Unemployment rate (EA-19) 1999M1–2019M12.
STOXX	Euro STOXX 1999M1–2019M12 (deflated by the HICP).
OILP	Brent Crude price FRED 1999M1–2019M12 (deflated by the HICP).

Table 1: Data

specifications. The external one serves as the baseline comparison, as it is the main reference in his work. Importantly, the conclusions remain robust across both specifications.[4]

7.2 The narrative sign restrictions

We leverage on Känzig (2024)'s instrument to identify the relevant dates for imposing the NSR. For this reason, we now describe the instrument.

The author constructs the instrument based on high-frequency data reflecting market responses to policy announcements under the EU ETS.[5] Specifically, the carbon policy surprise instrument is calculated as the change in European Union Allowances (EUA) futures prices on the regulatory event day, relative to the previous trading day's close. Since carbon prices were near zero at the end of the first phase of the ETS, the surprise instrument is scaled by the previous day's wholesale electricity price to ensure standardization in impact

[4] Including the instrument as the first variable in the VAR and identifying shocks using a Cholesky decomposition yields results consistent with the internal specification. In contrast, using the identified shock variable directly as the first variable and identifying shocks using a Cholesky decomposition replicates the external approach, as shown in Appendix 9

[5] Due to the establishment of the carbon market only in 2005, this instrument is available from that year onward. To address this limitation, missing values in the surprise series are set to zero.

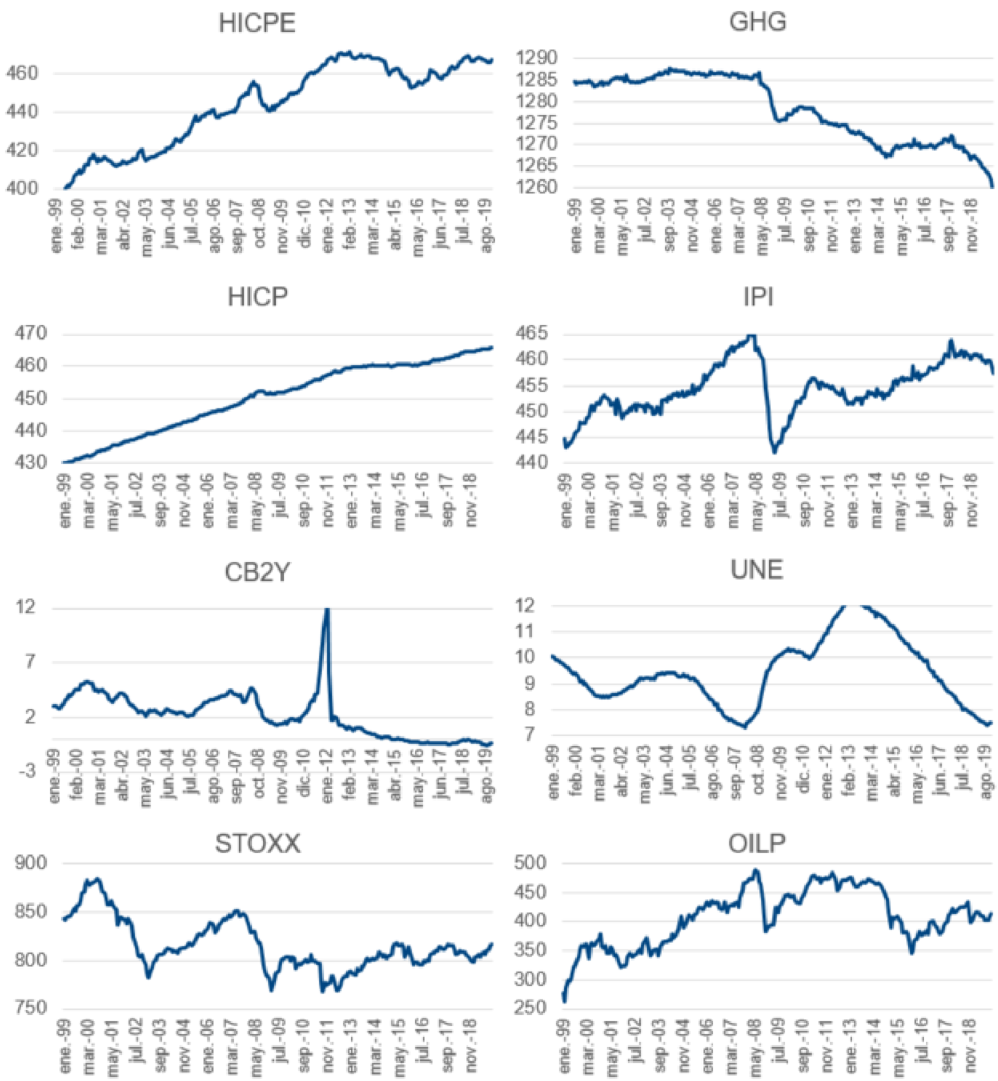

Figure 3: *Data Series.*

measurement.

The instrument is defined as follows:

$$CPSurprise_{t,d} = \frac{F^{\text{carbon}}_{t,d} - F^{\text{carbon}}_{t,d-1}}{p^{\text{elec}}_{t,d-1}},$$

where $F^{\text{carbon}}_{t,d}$ denotes the EUA futures price on day d, and $p^{\text{elec}}_{t,d-1}$ represents the wholesale electricity price on the previous day. The daily surprises are then aggregated to create a monthly series:

$$CPSurprise_t = \sum_{d=1}^{D} CPSurprise_{t,d}$$

where D is the number of trading days within the month. If no regulatory event occurs within a given month, the series takes a zero value, thus capturing only the policy-driven price adjustments.

Based on the NSR identification strategy, we isolate dates on which carbon pricing shocks are most likely to have occurred by focusing on episodes where Känzig's policy surprise registers a positive (negative) change, accompanied by a contemporaneous decline (increase) in GHG emissions. To ensure that these movements are not primarily driven by demand-side fluctuations, any simultaneous decrease (increase) in industrial production must be smaller in magnitude than the observed change in emissions.

The dates identified include: March 2011, February 2013, September 2013, February 2014, November 2018, February 2019, April 2019, July 2019, and August 2019. In total, we identified nine events, eight of which occurred during Phase 3 of the EU ETS -a period marked by a diminished role of free allocations and higher stability and credibility around the scheme. Figure 4 provides a visualization of these selected events. In particular, it shows the instrument (blue) and the selected events (red) for NSR identification.[6]

[6]Using these identified dates, we impose the restriction that shocks occurred at these dates and specify the sign of the j-th shock for episodes s_j, occurring at dates $t_1, \ldots, t_{s_j}$. If the instrument increases, the shocks are defined as positive.

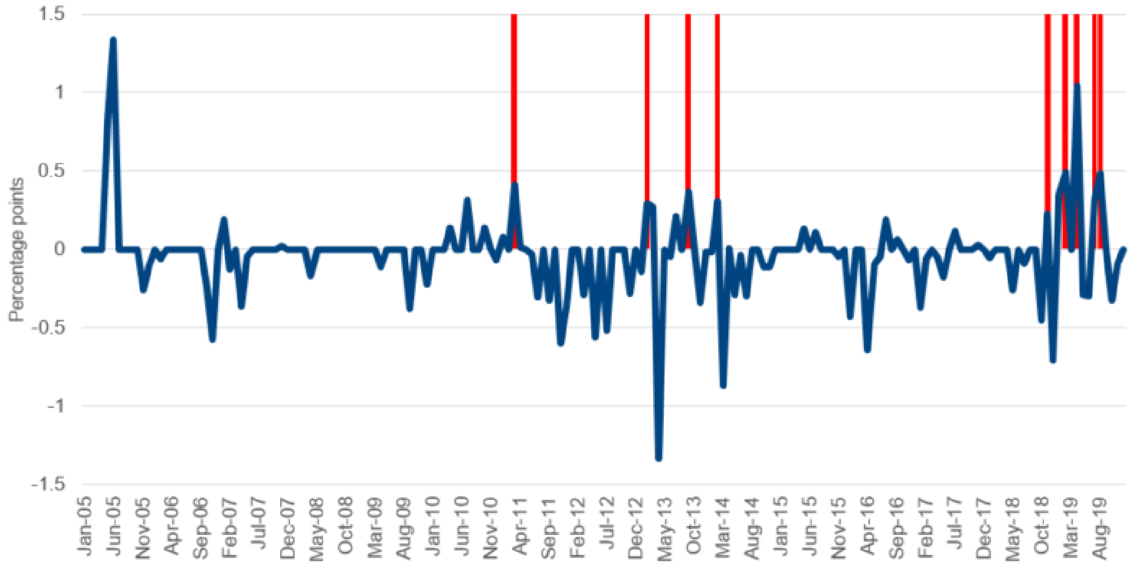

Figure 4: *The Carbon Policy Surprise Series (blue) and Selected Events (red).*

8 Results

We now present the empirical results, focusing on the impulse responses to a carbon price shock. The shock is normalized to generate a 1% increase in energy inflation. As shown below, our findings are broadly consistent with those of Känzig (2024), with one notable distinction: the use of NSR improves the interpretability of the responses by yielding a lower, and arguably more realistic, elasticity between IPI and GHG emissions. This estimate better reflects the historical decoupling trends discussed in section 2. As we show in the final part of this section, our approach allows for the construction of more plausible decarbonization scenarios.

8.1 Impulse Response Functions

Figure 5 displays the impulse response functions for GHG emissions and economic activity measured by IPI (dark blue) and compares them to the external instrument approach in

Känzig (2024)[7] (light blue). Both GHG emissions and IPI respond negatively to a positive carbon price shock, with emissions exhibiting a substantially larger decline. This highlights the critical importance of NSR in estimating an elasticity between IPI and emissions more in line with the recent improvements in energy and carbon intensity described in section 2. This can be seen in Figure 6. Additionally, industrial production declines contemporaneously with emissions, before stabilizing and partially recovering towards the end of the horizon.

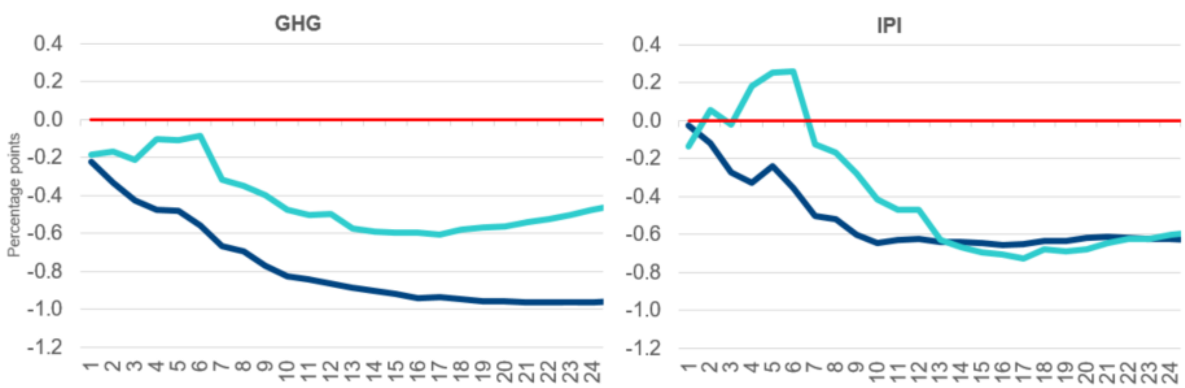

Figure 5: *IRFs to a positive carbon price shock for GHG and IPI. Our approach (dark blue) and Känzig (2024) (light blue).*

Returning to the analysis, Figure 6 shows that the mean elasticity -from period 9 to 24- of IPI to GHG emissions decreases from over 1.02 (with a maximum of 1.2) to approximately 0.65 (with a maximum of 0.68). This adjustment is particularly important given the ETS's growing influence on the energy sector in recent years, a domain where green technologies have gained considerable traction and energy efficiency improvements have been increasingly evident. Consequently, an elasticity of 0.65 appears more consistent with the structural shifts observed in the emission data and is arguably more plausible than the higher estimates reported in Känzig (2024).

[7] We replicate Kanzig's results by incoporating his estimated shock as the first variable in a VAR identified via Cholesky decomposition, which is equivalent to estimating a Proxy VAR using his policy surprise as an external instrument (see Annex 9). This approach is also employed to simulate the net-zero scenario in section 7.2, ensuring comparability with Kanzig's methodology.

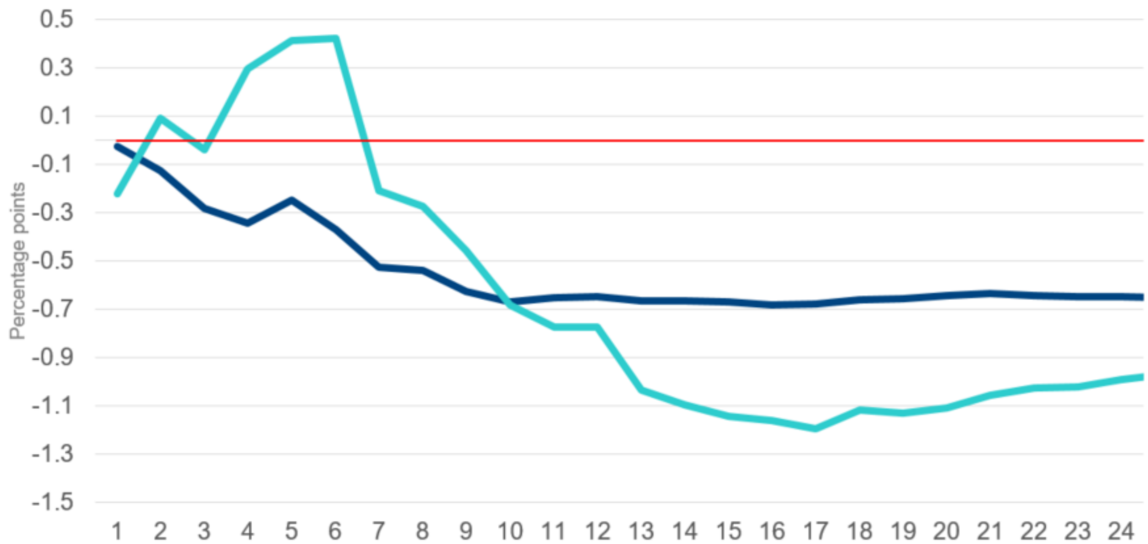

Figure 6: *Percentage of IPI change normalized to a maximum 1% decrease in GHG emissions. Our approach (dark blue) and Känzig (2024) (light blue).*

The results indicate that carbon price shocks have a more substantial impact on economic activity than previously estimated by earlier studies on other policy instruments applied in different contexts, such as Metcalf and Stock (2020) and Konradt and Weder di Mauro (2021), which generally find no significant negative effects on economic performance. However, this impact is smaller than that reported in recent literature on the EU-ETS, such as Känzig and Konradt (2023) and Känzig (2024), which document an elasticity close to one between emissions and economic activity. This divergence may reflect differences in both policy scope and identification strategies. Earlier studies primarily analyze marginal schemes with limited coverage relative to total emissions, while more recent approaches may be subject to confounding factors, such as overlapping macroeconomic shocks, that complicates the empirical identification of causal effects.

Figure 7 presents the remaining impulse response functions, highlighting the dynamic effects of a restrictive carbon policy shock. In particular, the shock leads to an immediate and pronounced increase in energy prices, accompanied by a significant and persistent decline in GHG emissions. These results underscore the effectiveness of carbon pricing in curbing emissions and contributing to climate change mitigation by raising the cost of carbon-intensive production.

From a macroeconomic perspective, the reduction in GHG emissions comes at a cost. IPI declines, and the unemployment rate increases. However, as previously noted, the decline in IPI is significantly smaller than in Känzig (2024), and arguably more consistent with expected outcomes. Consumer prices, as measured by the HICP, also rise in response to the shock. The pass-through effect is particularly pronounced for headline inflation, while core inflation experiences a more modest increase that proves to be short-lived.

Monetary policy appears to respond by counteracting inflationary pressures induced by the carbon price shock, potentially amplifying the adverse effects on economic activity. Unlike in Känzig (2024), stock prices exhibit a pronounced immediate decline but recover more quickly. In contrast, oil prices rise sharply, reflecting the inclusion of European oil producers and refineries within the scope of the emissions trading scheme.

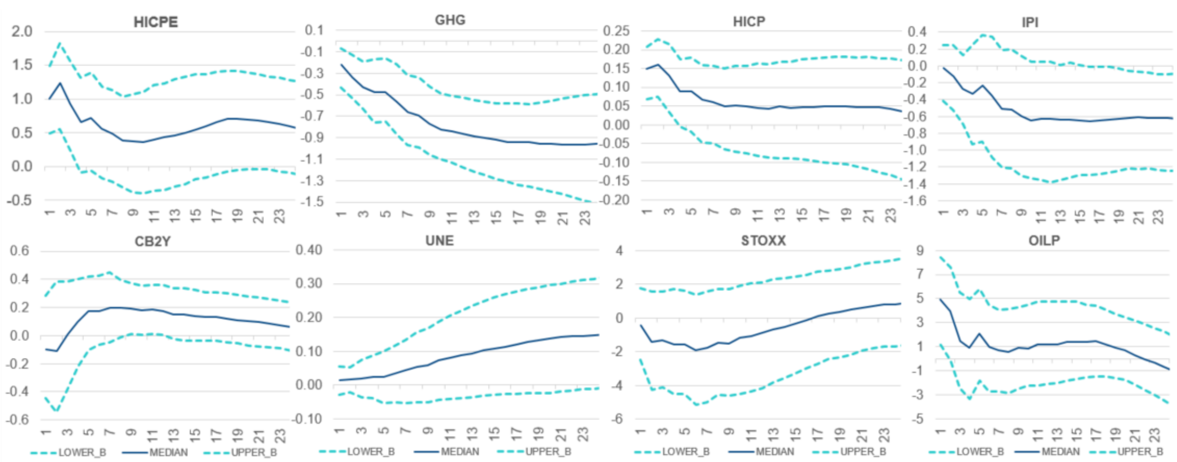

Figure 7: *IRFs for all the variables in the system. Mean and 68% confidence bands. Percentage points.*

In terms of magnitudes, a normalized carbon price shock results in GHG emissions and industrial production declining by approximately 1% and 0.6%, respectively. The unemployment rate increases by about 15 basis points, while consumer prices increase by slightly more than 0.15%. The two-year interest rate climbs by approximately 20 basis points, stock prices fall by roughly 2%, and oil prices increase by around 5% -all measured at the peak of their respective responses. These responses are both statistically and economically significant. While price effects materialize rapidly, the impacts on IPI and GHG emissions exhibit substantial lags, with their peaks occurring nearly two years after the initial shock.

Aside from the change in the IPI to GHG emissions elasticity, our impulse responses align broadly with those reported by Känzig (2024) as shown in Figure 8. The introduction of NSR slightly increases the uncertainty surrounding the magnitude of the estimated effects. Nevertheless, the responses remain statistically significant. Figure 8 also shows a slightly attenuated price response, consistent with the reduced impact on economic activity. This moderation is also reflected in a marginally lower unemployment rate. Similarly, as expected, the increase in oil prices is more contained, and the stock market correction proves less persistent.

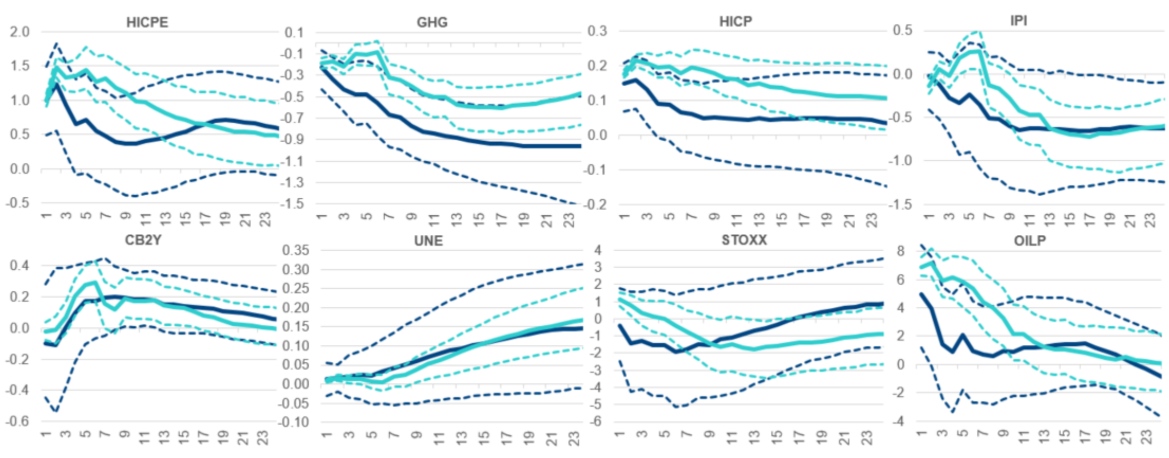

Figure 8: *IRFs for all the variables. Mean and 68% confidence bands. Our approach (dark blue) and Känzig (2024) (light blue). Percentage points.*

8.2 Net-Zero Transition Scenario

This section examines the potential economic effects of a net-zero transition scenario in the Eurozone, aligned with Phase IV of the Network for Greening the Financial System (NGFS).[8] Specifically, we calibrate the magnitude of the carbon price shock required to achieve the path of GHG emission embedded in the net-zero transition scenario of the NGFS, and evaluate the economic cost through its effect on the IPI from 2024 to 2026.

To quantify the implications of the scenario, it is important to point out that, over the three years considered in this section, the gap in cumulative GHG emissions between the NGFS net-zero scenario and the current policy scenario widens to seven percent.[9] Figure 9 shows the GHG emissions path under both scenarios (dark blue for the current policy and light blue for the net-zero transition scenario) with historical data until the end of 2023.

It is important to note that multiple net-zero pathways exist, and numerous potential combinations, including scenarios with declines occurring before or after those specified by the NGFS, are possible. For the purposes of this analysis, we adopt the NGFS's pathway. However, comparable conclusions would be obtained under alternative net-zero trajectories. The simulation results are computed using both our approach and that of Känzig (2024).

As Figure 10 shows, the simulation results indicate that, under our model, the economic adjustments required to achieve a net-zero emissions scenario are substantial. By the end of the three years, IPI is -3.9% below the level projected under the current policy scenario (dark blue for the current policy and light blue for the net-zero transition scenario). This result

[8]The NGFS is a coalition of central banks and supervisors advocating for the integration of climate-related considerations into financial practices. It provides climate scenarios to assess the economic impacts of various transition pathways.

[9]The NGFS net-zero scenario outlines a pathway to achieve global net-zero emissions by 2050, consistent with limiting global warming to 1.5°C. This scenario necessitates ambitious policies, such as stringent carbon pricing and accelerated deployment of green technologies. While these measures impose significant short-term economic adjustments, they effectively mitigate long-term climate risks. By contrast, the Current Policies scenario assumes no additional climate measures beyond those already implemented, leading to continued emissions growth and global warming exceeding 3°C by the end of the century. Although this scenario avoids immediate economic disruptions, it substantially heightens long-term climate and economic risks.

Figure 9: *GHG emissions. Net-zero (light blue) and Current Policies scenarios (dark blue).*

is consistent with the expected proportional relationship between emissions reductions and industrial activity, and it contrasts with the negligible macroeconomic impact reported by Metcalf and Stock (2020).

Figure 10: *IPI (index). Net-zero (light blue) and Current Policies scenarios (dark blue).*

Figure 11 compares the economic cost of achieving the net-zero emissions scenario under our identification strategy (light blue) and that of Känzig (2024) (red) for the net-zero emissions scenario. The results based on Känzig (2024) imply a substantially larger economic impact, culminating in a 12.9% decline in IPI by the end of the simulation horizon. This trajectory suggests that, if extended beyond 2026, the gap in industrial output between the two scenarios would continue to widen at an accelerated pace.

These findings underscore the importance of incorporating narrative information into the identification strategy, particularly to disentangle the effects of a carbon price shock from other concurrent demand-side disturbances. The results produced by our specification -a reduction in IPI slightly exceeding half the reduction in GHG emissions- appear more consistent with the empirical evidence and the data presented in section 2, including the protracted penetration of renewables in the energy mix and the improvement of energy efficiency per unit of GDP.

In contrast, the scenario implied by the Känzig (2024)'s identification approach -where the decline in IPI exceeds twice the reduction in emissions- would render a net-zero transition economically implausible under current structural conditions.

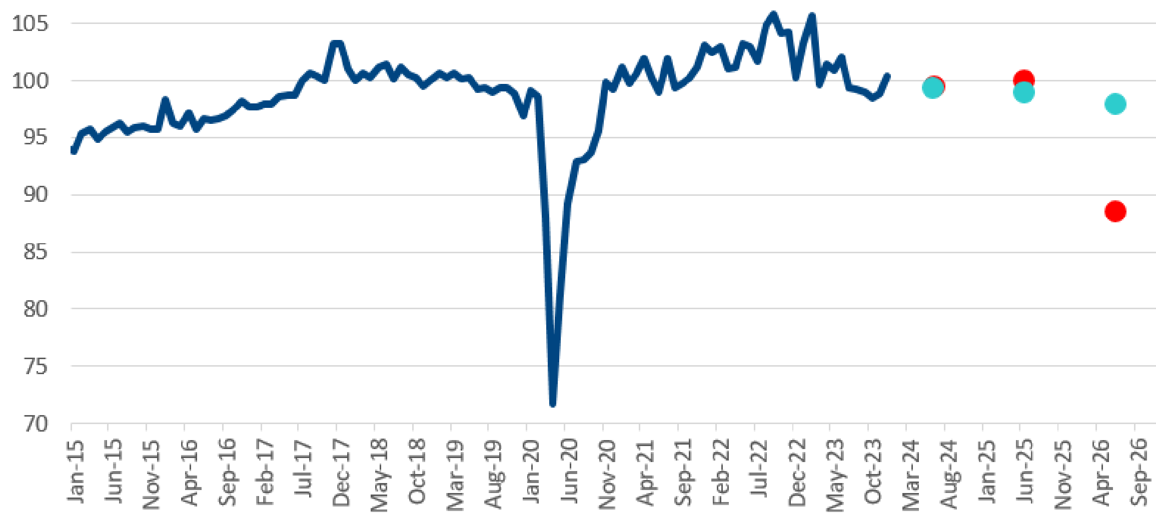

Figure 11: *IPI (index). Net-zero scenario. Our approach (light blue) and Känzig (2024) (red).*

9 Conclusion

The transition to a low-carbon economy is one of the most critical economic and environmental challenges of our time. While global efforts have often faced political and institutional hurdles, individual countries have increasingly implemented carbon pricing mechanisms to reduce emissions domestically. Despite the growing adoption of these policies, their broader economic and environmental effects remain insufficiently understood. This paper contributes to filling this gap by analyzing the EU ETS, the world's largest carbon market.

Our findings show that stricter carbon pricing policies effectively drive higher energy prices and sustained reductions in GHG emissions. However, these benefits come with transitional costs, including slower economic activity and a temporary increase in inflation.

This paper advances our understanding of the macroeconomic implications of carbon pricing by applying NSR within a SVAR framework. The NSR approach provides two key advantages. First, it eliminates the need for an explicit shock series by focusing solely on identifying pivotal regulatory events, while incorporating safeguards to exclude episodes potentially confounded by unrelated negative demand shocks. Second, it produces empirically robust results that align more closely with theoretical predictions and observed emission and green technology trends, particularly in quantifying the elasticity of GHG emissions reductions relative to industrial production fluctuations.

On the one hand, our findings indicate that carbon price shocks have a more substantial impact on economic activity than suggested by earlier studies on other policy instruments applied in different contexts, such as Metcalf and Stock (2020) and Konradt and Weder di Mauro (2021), which generally find no significant negative effects on economic performance. On the other hand, our results challenge previous conclusions that decarbonization would necessitate near-total economic collapse, often implying a counterintuitive one-to-one elasticity between GHG emissions reduction and IPI when analyzing the impact of the EU-ETS -see Känzig and Konradt (2023) or Känzig (2024)-.

Instead, our work suggests that GHG emissions reductions can be achieved alongside significant, but more moderate, declines in IPI. This indicates that while the economic costs of decarbonization are considerable, they do not lead to the total collapse of economic activity. Nevertheless, the economic costs identified in our results remain notable, emphasizing the need for unprecedented technological innovation to meet ambitious decarbonization targets. Simply put, the pace of innovation will need to surpass anything observed to date.

In conclusion, the NSR methodology not only simplifies the analysis of carbon pricing impacts but also enhances the robustness and applicability of the findings. Future research should extend this approach to other carbon markets and explore its potential in evaluating a wider array of climate policies.

References

ANDERSSON, J. (2019): "Carbon Taxes and CO2 Emissions: Sweden as a Case Study," *American Economic Journal: Economic Policy*.

ANTOLÍN-DÍAZ, J. AND J. F. RUBIO-RAMÍREZ (2018): "Narrative Sign Restrictions for SVARs," *American Economic Review*, 108, 2802–29.

ARIAS, J. E., J. F. RUBIO-RAMÍREZ, AND D. F. WAGGONER (2018): "Inference Based on Structural Vector Autoregressions Identified With Sign and Zero Restrictions: Theory and Applications," *Econometrica*, 86, 685–720.

BERNARD, J.-T. AND M. KICHIAN (2021): "The Impact of a Revenue-Neutral Carbon Tax on GDP Dynamics: The Case of British Columbia," *Energy Journal*.

BERTHOLD, L. ET AL. (2023): "The Heterogeneous Effects of Carbon Pricing: Macro and Micro Evidence," *CFM Discussion Papers*.

CANOVA, F. AND G. D. NICOLO (2002): "Monetary disturbances matter for business fluctuations in the G-7," *Journal of Monetary Economics*, 49, 1131–1159.

COMMISSION, E. (2025): "EU Emissions Trading System (EU ETS)," .

FAUST, J. (1998): "The robustness of identified VAR conclusions about money," International Finance Discussion Papers 610, Board of Governors of the Federal Reserve System (U.S.).

GOULDER, L. H. AND M. A. HAFSTEAD (2018): *Confronting the Climate Challenge: U.S. Policy Options*, Columbia University Press.

HENSEL, D. ET AL. (2024): "Carbon Pricing and Inflation Expectations: Evidence from France," *Journal of Monetary Economics*.

Konradt, M. and B. Weder di Mauro (2021): "Carbon Taxation and Greenflation: Evidence from Europe and Canada," *IHEID Working Papers*.

Känzig, D. R. (2024): "The Unequal Economic Consequences of Carbon Pricing," *National Bureau of Economic Research Working Paper*.

Känzig, D. R. and M. Konradt (2023): "Climate Policy and the Economy: Evidence from Europe's Carbon Pricing Initiatives," *National Bureau of Economic Research Working Paper*.

Martin, R., L. B. De Preux, and U. Wagner (2014): "The Impact of a Carbon Tax on Manufacturing: Evidence from Microdata," *Universidad Carlos III de Madrid Archive*.

McKibbin, W. J. et al. (2017): "Climate Change and Monetary Policy: Dealing with Disruption," *Brookings Institution*.

Metcalf, G. E. (2019): "On the Economics of a Carbon Tax for the United States," *Brookings Papers on Economic Activity*, Spring, 405–458.

Metcalf, G. E. and J. H. Stock (2020): "Measuring the Macroeconomic Impact of Carbon Taxes," *American Economic Review: Papers and Proceedings*.

Moore, F. C., M. A. Drupp, J. Rising, S. Dietz, I. Rudik, and G. Wagner (2024): "Synthesis of evidence yields high social cost of carbon due to structural model variation and uncertainties," *Proceedings of the National Academy of Sciences*, 121, e2410733121.

Ohlendorf, N. et al. (2021): "Distributional Impacts of Carbon Pricing: A Meta-Analysis," *Environmental and Resource Economics*.

Pindyck, R. S. (2022): *Climate Future: Averting and Adapting to Climate Change*, Columbia University Press.

Project, G. C. (2024): “Global Carbon Budget 2024,” .

Rubio-Ramirez, J. F., D. F. Waggoner, and T. Zha (2010): “Structural Vector Autoregressions: Theory of Identification and Algorithms for Inference,” *Review of Economic Studies*, 77, 665–696.

Tracker, C. A. (2024): “CAT Emissions Gap 2024,” .

Uhlig, H. (2005): “What are the effects of monetary policy on output? Results from an agnostic identification procedure,” *Journal of Monetary Economics*, 52, 381–419.

Annex I. Algebraic Demonstration: Proxy VAR vs Cholesky Decomposition

1. Basic VAR Model

A VAR model can be written as:

$$\mathbf{y}_t = \mathbf{A}_0^{-1}\mathbf{e}_t,$$

where:

- $\mathbf{y}_t$ is the vector of endogenous variables.
- $\mathbf{A}_0^{-1}$ is the contemporaneous impact matrix.
- $\mathbf{e}_t$ is the vector of structural shocks ($\mathbf{e}_t \sim \mathcal{N}(0, \mathbf{I})$).

The reduced form is:

$$\mathbf{y}_t = \mathbf{A}(L)\mathbf{y}_{t-1} + \mathbf{u}_t,$$

where $\mathbf{u}_t = \mathbf{A}_0^{-1}\mathbf{e}_t$ are the reduced-form residuals ($\mathbf{u}_t \sim \mathcal{N}(0, \mathbf{\Sigma}_u)$).

2. Cholesky Decomposition

In a Cholesky decomposition, the covariance matrix of the reduced-form residuals, $\mathbf{\Sigma}_u$, is decomposed as:

$$\mathbf{\Sigma}_u = \mathbf{P}\mathbf{P}^\top,$$

where $\mathbf{P}$ is a lower triangular matrix representing the contemporaneous effects of structural shocks on the variables.

Under this decomposition, we assume:

1. The first shock is exogenous and contemporaneously affects all other variables.

2. Subsequent shocks do not contemporaneously affect the first shock.

The contemporaneous impact matrix becomes:

$$\mathbf{A}_0^{-1} = \mathbf{P}.$$

3. Proxy VAR with an Estimated External Shock

In a proxy VAR, we use an external instrument z_t that satisfies the following conditions:

- $\mathbb{E}[z_t \cdot e_{1t}] \neq 0$: The instrument is correlated with the structural shock of interest.

- $\mathbb{E}[z_t \cdot e_{jt}] = 0$ for all $j \neq 1$: The instrument is uncorrelated with other shocks.

The instrument is used to directly identify the first structural shock (e_{1t}). If we estimate this shock as $\hat{e}_{1t}$, it is treated as given. This is equivalent to introducing it as the first exogenous variable in a VAR.

The reordered system becomes:

$$\begin{bmatrix} \hat{e}_{1t} \\ \mathbf{y}_t^{(2)} \end{bmatrix} = \mathbf{A}_0^{-1} \begin{bmatrix} e_{1t} \\ \mathbf{e}_t^{(2)} \end{bmatrix}.$$

Where:

- $\hat{e}_{1t}$ is not contemporaneously affected by $\mathbf{y}_t^{(2)}$.

- This is exactly the assumption made in a Cholesky decomposition when placing the identified shock as the first variable.

4. Algebraic Equivalence

In both cases (Cholesky and Proxy VAR):

- The first row of $\mathbf{A}_0^{-1}$ will have zeros for all columns except the first (the most exogenous variable).
- Subsequent variables are contemporaneously conditioned on the first.

Thus, the system is equivalent to:

$$\mathbf{y}_t = \begin{bmatrix} \hat{e}_{1t} \\ \mathbf{y}_t^{(2)} \end{bmatrix},$$

where the first identified shock operates exogenously, and the other variables adjust conditionally.

Thus, by placing the identified shock ($\hat{e}_{1t}$) as the first variable in a VAR, the procedure is algebraically equivalent to applying a Cholesky decomposition with the identified shock as the most exogenous variable. This ensures that it is not contemporaneously affected by other variables.

Working papers

2025

25/04 **Joxe Mari Barrutiabengoa Ortubai, Rodrigo Enrique Falbo Piacentini, Agustín García Serrador, Juan F. Rubio-Ramírez:** Unraveling the impact of a carbon price shock on macroeconomic variables: a Narrative Sign Restrictions approach.

25/03 **Alvaro Ortiz, Tomasa Rodrigo, David Sarasa, Pedro Torinos, Sirenia Vazquez:** What can 240,000 new credit transactions tell us about the impact of NGEU funds?.

25/02 **Gergely Buda, Vasco M. Carvalho, Giancarlo Corsetti, João B. Duarte, Stephen Hansen, Afonso S. Moura, Álvaro Ortiz, Tomasa Rodrigo, José V. Rodríguez Mora, Guilherme Alves da Silva:** The Short Lags of Monetary Policy.

25/01 **Ángel de la Fuente:** Series largas de algunos agregados económicos y demográficos regionales: actualización de RegData hasta 2023.

2024

24/14 **Joxe M. Barrutiabengoa, Giancarlo Carta, Nara González, Pilar Más, Diego Pérez, Gül Yücel:** The Impact of Climate Change on Tourism Demand in Türkiye.

24/13 **Clodomiro Ferreira, José Miguel Leiva, Galo Nuño, Álvaro Ortiz, Tomasa Rodrigo and Sirenia Vazquez:** The heterogeneous impact of inflation on households' balance sheets.

24/12 **Ángel de la Fuente:** La evolución de la financiación de las comunidades autónomas de régimen común, 2002-2022.

24/11 **J.M. Barrutiabengoa, G. Carta, N. González, D. Pérez, P. Más and G. Yücel:** Climate change scenarios and the evolution of Spanish tourism.

24/10 **Federico D. Forte:** Pronóstico de inflación de corto plazo en Argentina con modelos *Random Forest*.

24/09 **Ángel de la Fuente:** La liquidación de 2022 del sistema de financiación de las comunidades autónomas de régimen común.

24/08 **Prachi Mishra, Alvaro Ortiz, Tomasa Rodrigo, Antonio Spilimbergo, and Sirenia Vazquez:** E-commerce during Covid in Spain: One "Click" does not fit All.

24/07 **A. Castelló-Climent and R. Doménech:** Convergence in Human Capital and Income.

24/06 **J. Andrés, J.E. Boscá, R. Doménech and J. Ferri:** TheWelfare Effects of Degrowth as a Decarbonization Strategy.

24/05 **Ángel de la Fuente:** Las finanzas autonómicas en 2023 y entre 2003 y 2023.

24/04 **Ángel de la Fuente y Pep Ruiz:** Series largas de VAB y empleo regional por sectores, 1955-2022. Actualización de RegData-Sect hasta 2022.

24/03 **Ángel de la Fuente:** Series largas de algunos agregados económicos y demográficos regionales: Actualización de RegData hasta 2022.

24/02 **J. Andrés, E. Bandrés, R. Doménecha and M.D. Gadea:** SocialWelfare and Government Size.

24/01 **J. Andrés, J.E. Boscá, R. Doménech and J. Ferri:** Transitioning to net-zero: macroeconomic implications and welfare assessment.

CLICK HERE TO ACCESS THE WORKING DOCUMENTS PUBLISHED IN

Spanish and English

DISCLAIMER

The present document does not constitute an “Investment Recommendation”, as defined in Regulation (EU) No 596/2014 of the European Parliament and of the Council of 16 April 2014 on market abuse (“MAR”). In particular, this document does not constitute “Investment Research” nor “Marketing Material”, for the purposes of article 36 of the Regulation (EU) 2017/565 of 25 April 2016 supplementing Directive 2014/65/EU of the European Parliament and of the Council as regards organisational requirements and operating conditions for investment firms and defined terms for the purposes of that Directive (MIFID II).

Readers should be aware that under no circumstances should they base their investment decisions on the information contained in this document. Those persons or entities offering investment products to these potential investors are legally required to provide the information needed for them to take an appropriate investment decision.

This document has been prepared by BBVA Research Department. It is provided for information purposes only and expresses data or opinions regarding the date of issue of the report, prepared by BBVA or obtained from or based on sources we consider to be reliable, and have not been independently verified by BBVA. Therefore, BBVA offers no warranty, either express or implicit, regarding its accuracy, integrity or correctness.

This document and its contents are subject to changes without prior notice depending on variables such as the economic context or market fluctuations. BBVA is not responsible for updating these contents or for giving notice of such changes.

BBVA accepts no liability for any loss, direct or indirect, that may result from the use of this document or its contents.

This document and its contents do not constitute an offer, invitation or solicitation to purchase, divest or enter into any interest in financial assets or instruments. Neither shall this document nor its contents form the basis of any contract, commitment or decision of any kind.

ENQUIRIES TO::
BBVA Research: Azul Street. 4. La Vela Building – 4th and 5th floor. 28050 Madrid (Spain).
Tel.:+34 91 374 60 00 y +34 91 537 70 00 / Fax:+34 91 374 30 25
www.bbvaresearch.com